Published in IET Control Theory and Applications
Received on 28th October 2009
Revised on 23rd February 2010
doi: 10.1049/iet-cta.2009.0558

ISSN 1751-8644

Discrete time integral sliding mode control for overhead crane with uncertainties

Z. Xi T. Hesketh

School of Electrical Engineering and Telecommunications, University of New South Wales, Australia
E-mail: xixicat0513@gmail.com

Abstract: This study firstly addresses an integral sliding mode control method for discrete time systems. The underlying continuous system is affected by both matched and unmatched uncertainties. The past value of the disturbance signal is taken as the estimate of its present value. The sliding mode controller is designed to ensure the existence of sliding mode in the presence of uncertainties. The proportional part is designed based on the analysis of closed-loop stability conditions. The controller design theory above is applied to an overhead crane system in later sections. The overhead crane system, which is a familiar control problem is described by a linear model, the parameters of which are estimated. It is affected by uncertainties such as friction, swing of the load and non-linearities because of changing rope length. Both simulation and experimental results are reported. The efficacy and robustness of the proposed controller are demonstrated.

1 Introduction

Overhead travelling cranes are widely used in industry for the transfer of heavy loads. It is highly desirable that the load is transferred to a specified position with high speed, minimum swing and precision of the destination. Hence, the overhead crane has been a popular subject for control studies for many years. In [1], a non-linear controller is designed based on a non-linear model of the overhead crane, whereas Sakawa and Sano developed a linear controller for a non-linear model in [2]. A methodology for the design of a robust feedforward/feedback control for crane system based on dynamic inversion was proposed in 1997 [3] and Chang designed an adaptive fuzzy control for overhead crane system that considers the disturbance effect. In both industrial and laboratory processes [4], the degradation of the system performance because of uncertain factors cannot be ignored. For the overhead crane systems, the existence of uncertainties because of the change in the length of the lift rope, changing mass of the payload and external disturbances is inevitable. In this paper, we report an integral sliding mode (ISM) controller for discrete time systems with uncertainties for application to the overhead crane (laboratory process) system. The motivation for developing discrete control laws is the fact that controllers are implemented with finite sampling interval even if they are designed in continuous time frame and the finite step size always leads to degradation of the performance of continuous controllers. A controller based on a discrete time models is appropriate. It is emphasised here that the system model used in this paper is linear and is derived from system identification, permitting rapid implementation on different cranes.

Variable structure systems (VSS) have been extensively used for control of dynamic industrial processes. The essence of variable structure control (VSC) is to use a high-speed switching control scheme to drive the plant's state trajectory onto a specified and user chosen surface in the state space which is commonly called the sliding surface or switching surface and then to keep the plant's state trajectory moving along this surface [5–7]. One of the advantages of sliding mode control is robustness. However, before the sliding surface is reached, the system is not insensitive to noise and uncertainties. Discrete sliding mode has also been addressed in [8].

In [9], Utkin and Shi proposed an improved sliding control method named 'integral sliding mode control (ISMC)'. Subsequently, ISM has received a lot of

attention. Wang *et al.* introduced new methods for designing ISM controllers [10]. Ackermann's formula was applied to design reduced and full order sliding mode controllers by Ackermann and Utkin [11]. Moreover, integral sliding surface designs were developed for systems with matched and unmatched uncertainties [12, 13]. In contrast with conventional sliding mode control, the system motion under ISM has a dimension equal to that of the state space. In ISMC, the system trajectory always starts from the sliding surface. Accordingly, the reaching phase is eliminated and robustness in the whole state space is promised. This is the reason that it is used for overhead crane system which requires superior robustness.

In the existing literature, the concept of ISM has not been as widely applied to discrete time systems. Wang *et al.* reported about discretisation of normal sliding mode systems in [14] and in 2007, Abidi *et al.* reported the design of discrete time ISMC [15]. They worked on a sampled data system whose continuous counterpart contained a matched uncertainty. An equivalent control law was established based on the assumption that the initial state was accurately known.

The contribution of Section 3 of this paper is to extend the design of discrete ISM systems to deal with both matched and unmatched uncertainties, which might arise for imperfect modelling and external disturbances. It is noticed that the discrete time counterpart of the matched uncertainty is not matched to the input any more. However, it can still be treated as a matched uncertainty after an approximation. In [16], the assumption that the uncertainties are continuous and smooth in time is made. If this is the case, the past value of the disturbance signal can be taken as the expectation of its present value, leading to the result that the deviation of the sliding variable from zero is $O(T^2)$. Owing to the existence of this deviation, even the matched uncertainty cannot be cancelled completely, yet the trajectory stays within a certain bound around the sliding surface and the sliding mode is maintained with a controller to suppress the effect of the uncertainties. The result of closed-loop analysis shows that closed-loop stability is achieved with a proper set of design parameters and the convergence of the states to the origin is also guaranteed. Furthermore, our controller contains a term which ensures the trajectory will return to the sliding surface should it leave it for any reason. It is noticed that only single-input-single-output (SISO) system is considered in this paper but the results may be extended to multi-variable case with care.

The paper is organised as follows. The problem formulation is presented in Section 2 after the introduction in Section 1. In Section 3, the theory of controller design procedure is stated in detail. Section 4 is devoted to the application of the ISMC on overhead crane system and Section 5 concludes the paper.

2 ISMC problem statement

Consider a SISO continuous-time linear system of the form

$$\dot{x}(t) = \bar{A}x(t) + (\bar{B} + \Delta\bar{B})[u(t) + \bar{f}_{\mathrm{m}}(x,t)] + \bar{f}_{\mathrm{cu}}(x,t) \tag{1}$$

where $x(t) \in R^n$ is the state vector, $u \in R$ is the control input, and $\bar{f}_{\mathrm{m}}$ and $\bar{f}_{\mathrm{cu}}$ are matched and unmatched uncertainties, respectively. $\bar{A}$, $\bar{B}$, are known matrices or vectors of proper dimensions and n is also known. $\Delta\bar{B}$ represents the modelling error, assumed to be unknown but bounded. $\bar{f}_{\mathrm{m}}$ and $\bar{f}_{\mathrm{cu}}$ are additional disturbance signals which are assumed smooth and bounded. For such a system, the uncertainty caused by modelling error could be treated as part of the total unmatched uncertainty. Then the system model can be simplified as

$$\dot{x}(t) = \bar{A}x(t) + \bar{B}[u(t) + \bar{f}_{\mathrm{m}}(x,t)] + \bar{f}_{\mathrm{u}}(x,t) \tag{2}$$

with

$$\bar{f}_{\mathrm{u}}(x,t) = \bar{f}_{\mathrm{cu}}(x,t) + \Delta\bar{B}[u(t) + \bar{f}_{\mathrm{m}}(x,t)]$$

It is not hard to see that $\bar{f}_{\mathrm{u}}(x,t)$ is also bounded and smooth.

The corresponding discrete time description of (2) is

$$x(k+1) = Ax(k) + Bu(k) + \tilde{f}_{\mathrm{m}}(k) + f_{\mathrm{u}}(k) \tag{3}$$

where, for a sampling interval T

$$A = e^{\bar{A}T}, \quad B = \int_0^T e^{\bar{A}\tau}\,\mathrm{d}\tau\bar{B} \tag{4}$$

$$\tilde{f}_{\mathrm{m}}(k) = \int_0^T e^{\bar{A}\tau}\bar{B}\bar{f}_{\mathrm{m}}((k+1)T - \tau)\,\mathrm{d}\tau \tag{5}$$

$$f_{\mathrm{u}}(k) = \int_0^T e^{\bar{A}\tau}\bar{f}_{\mathrm{u}}((k+1)T - \tau)\,\mathrm{d}\tau \tag{6}$$

As mentioned in [13], if the uncertainty $\bar{f}_{\mathrm{m}}(x,t)$ is smooth and bounded, we have

$$\tilde{f}_{\mathrm{m}}(k) = \int_0^T e^{\bar{A}\tau}\bar{B}\bar{f}_{\mathrm{m}}((k+1)T - \tau)\,\mathrm{d}\tau = B\bar{f}_{\mathrm{m}}(k) + \frac{1}{2}Bv_{\mathrm{m}}(k)T + O(T^3) \tag{7}$$

with $v_{\mathrm{m}}(k) = (\mathrm{d}(\bar{f}_{\mathrm{m}})/\mathrm{d}t)(kT)$.

With (7), (3) can be written as

$$x(k+1) = Ax(k) + B(u(k) + f_{\mathrm{m}}(k)) + f_{\mathrm{u}}(k) \tag{8}$$

where $f_{\mathrm{m}}(k) = \bar{f}_{\mathrm{m}}(k) + (1/2)v_{\mathrm{m}}(k)T$, with an error $\varepsilon = O(T^3)$. It is assumed that B is full rank and it should be noticed that both $f_{\mathrm{m}}(k)$ and $f_{\mathrm{u}}(k)$ are bounded because of

doi: 10.1049/iet-cta.2009.0558

the boundedness of $\bar{f}_m$ and $\bar{f}_u$. Here, we have

$$0 \le \|f_m(k)\| \le F_m \le \infty \quad 0 \le \|f_u(k)\| \le F_u \le \infty \tag{9}$$

In this paper, $\| * \|$ is used to represent the Euclidean norm of $*$.

Remark 1: Most processes have underlying continuous behaviour. However, a discrete linear model may be derived from suitable parameter estimation.

3 Integral sliding mode controller design

3.1 Sliding surface design

A discrete-time integral sliding surface is [15]

$$\sigma(k) = Gx(k) - Gx(0) + h(k) = 0 \tag{10}$$

where $h(k)$ is iteratively computed as

$$h(k) = h(k-1) - (GBu_0(k-1) + GAx(k-1)) \tag{11}$$

where $\sigma \in R$, $h \in R$, $h(0) = 0$, $G \in R^{1\times n}$ is to be decided, $u_0(k) = -Kx(k)$ and the gain K is to be designed in a later section. $\sigma(k)$ represents the sliding variable in this paper.

According to (8), (10) and (11), we have

$$\sigma(k+1) = GB(u(k) + f_m(k)) + Gf_u(k) - Gx(0) + h(k) - GBu_0(k) \tag{12}$$

With the assumption that

$$u(k) = u_0(k) + u_1(k) \tag{13}$$

we have

$$\sigma(k+1) = GBu_1(k) + GBf_m(k) + Gf_u(k) + h(k) - Gx(0) \tag{14}$$

According to [16], the last value of a disturbance signal can be taken as the estimate of its current value if the updated value is not accessible, under the assumption that the disturbance is continuous and smooth. In this case, we have

$$f_m(k) - \hat{f}_m(k) \cong f_m(k) - f_m(k-1) = O(T^2) \tag{15}$$

$$f_u(k) - \hat{f}_u(k) \cong f_u(k) - f_u(k-1) = O(T^2) \tag{16}$$

with $\widehat{f_{m,u}}(k)$ representing the estimation of $f_{m,u}(k)$.

3.2 Sliding mode controller design

From (10) and (14), it can be seen that

$$\sigma(k+1) - \sigma(k) = GBu_1(k) + GBf_m(k) + Gf_u(k) - Gx(k) \tag{17}$$

Remark 2: For a discrete time system, the following conditions must be satisfied to guarantee the existence of sliding mode and to reduce the chattering effect:

1. $\sigma(k)(\sigma(k+1) - \sigma(k)) < 0$ so that the trajectory moves monotonically towards the sliding surface

2. $|\sigma(k+1)| \le |\sigma(k)|$ so that the size of successive chattering steps is non-increasing.

From (9), one can see that $\|(GB)(f_m(k) - \hat{f}_m(k))\| \le 2\|(GB)\|F_m$ and $\|G(f_u(k) - \hat{f}_u(k))\| \le 2\|G\|F_u$. Letting

$$2\|(GB)\|F_m = M, \quad 2\|G\|F_u = N \tag{18}$$

we have

$$\|(GB)(f_m(k) - \hat{f}_m(k))\| \le M\|, \quad G(f_u(k) - \hat{f}_u(k))\| \le N \tag{19}$$

Proposition 1: Let $Q(k) = (GB)(f_m(k) - \hat{f}_m(k) + G(f_u(k) - \hat{f}_u(k))$. Under the assumption that GB is invertible (G can be arbitrarily chosen as far as this assumption is met. One is reminded that B is assumed to be of full rank in Section 2.), the integral sliding mode controller can be designed as

$$u_1(k) = -(GB)^{-1}[GB\hat{f}_m(k) + G\hat{f}_u(k) - Gx(k) + \alpha(k)\sigma(k) + \beta(k)\mathrm{sgn}(\sigma(k))] \tag{20}$$

where we have the following (see equation at the bottom of the page)

As a result, a quasi-sliding mode [10] is realised.

Proof:

I. While $\sigma(k) \neq 0$.

$$\left\{ \begin{array}{l} \alpha(k) = 0 \\ \beta(k) = 0 \end{array} \right\}, \quad \text{when } \sigma(k) = 0$$

$$\left\{ \begin{array}{rl} \alpha(k) = \gamma(k)\mathrm{sgn}(\sigma(k)) + \epsilon, & \text{with } \gamma(k) = \dfrac{M+N}{|\sigma(k)|} \quad \text{and} \quad 0 < \epsilon < 1 \\ \beta(k) = \lambda|(1-\epsilon)\sigma(k)|, & \text{with } 0 < \lambda < 1 \end{array} \right\} \text{otherwise}$$

Substitute (20) back into (17)

$$\sigma(k+1)-\sigma(k)=-\alpha(k)\sigma(k)-\beta(k)\mathrm{sgn}(\sigma(k)) + (GB)(f_{\mathrm{m}}(k)-\widehat{f}_{\mathrm{m}}(k))+G(f_{\mathrm{u}}(k)-\widehat{f}_{\mathrm{u}}(k)) \tag{21}$$

Hence

$$\sigma(k)(\sigma(k+1)-\sigma(k)) = -\alpha(k)\sigma^2(k)-\beta\sigma(k)\mathrm{sgn}(\sigma(k))+Q(k)\sigma(k) \tag{22}$$

$$= \sigma(k)[Q(k)-\alpha(k)\sigma(k)-\beta(k)\mathrm{sgn}(\sigma(k))] \tag{23}$$

As (18) and (19) imply

$$Q(k) < |Q(k)| < M+N = \gamma(k)|\sigma(k)|$$

Hence, it can be seen from (23) that $\sigma(k)(\sigma(k+1)-\sigma(k)) < 0$ provided $\alpha(k) > 0$ for any non-zero $\sigma(k)$.

Furthermore, from (17) we have

$$\sigma(k+1)=(\sigma(k)+Q(k)-\alpha(k)\sigma(k))-\beta(k)\mathrm{sgn}(\sigma(k))$$

then

$$\begin{aligned}|\sigma(k+1)| &= |(1-\alpha(k))\sigma(k)+(\gamma(k)|\sigma(k)|-\varsigma)-\beta(k)\mathrm{sgn}(\sigma(k))|\\ &= |(1-\alpha(k))\sigma(k)+(\gamma(k)\mathrm{sgn}(\sigma(k))\sigma(k)-\varsigma)\\ &\quad -\beta(k)\mathrm{sgn}(\sigma(k))|\\ &= |(1-\epsilon)\sigma(k)-\varsigma-\beta(k)\mathrm{sgn}(\sigma(k))|\end{aligned}$$

with $\varsigma=\gamma(k)|\sigma(k)|-Q(k)=M+N-Q(k)$.

So

$$\begin{aligned}|\sigma(k+1)| &= |(1-\epsilon)\sigma(k)-\varsigma-\lambda|(1-\epsilon)\sigma(k)|\mathrm{sgn}(\sigma(k))|\\ &= |(1-\lambda)(1-\epsilon)\sigma(k)-\varsigma|\end{aligned}$$

It is seen from above that when $\sigma(k) < -(\varsigma/(\lambda+\epsilon-\lambda\epsilon))$ or $\sigma(k) > (\varsigma/(2-(\lambda+\epsilon-\lambda\epsilon)))$, $|\sigma(k+1)| < |\sigma(k)|$ is satisfied. It should be noted that for the case $\sigma(k) < 0$, there is another condition to ensure $\sigma(k)(\sigma(k+1)-\sigma(k)) < 0$, which is $\alpha(k) > 0$. According to Proposition 1, $\alpha(k)=\gamma(k)\mathrm{sgn}(\sigma(k))+\epsilon$, with $0 < \varepsilon < 1$. Therefore it is necessary to have

$$\gamma(k)=\frac{M+N}{|\sigma(k)|} \tag{24}$$

to guarantee the positiveness of $\alpha(k)$. Equation (24) implies the second condition on $\sigma(k)$ to promise the size of $\sigma(k)$ decreases when $\sigma(k) < 0$, which is $\sigma(k) < -(M+N)$. Considering the fact that $\varsigma=M+N-Q(k)$ and $Q(k) < \|Q(k)\| < M+N$, we have $0 < \varsigma < 2(M+N)$. Then we can conclude that $\sigma(k)$ exhibits a quasi-sliding mode. The lower and upper bounds ($\bar{U}_{\mathrm{l}}$ and $\bar{U}_{\mathrm{u}}$, respectively) of the quasi-sliding mode band $U_{\mathrm{l}} \le \sigma(k) \le U_{\mathrm{u}}$ are defined below

$$U_{\mathrm{l}} > \bar{U}_{\mathrm{l}} = \min\left(-\frac{2(M+N)}{l},\ -(M+N)\right)$$

$$U_{\mathrm{u}} < \bar{U}_{\mathrm{u}} = \frac{2(M+N)}{2-l} \quad \text{with } l=\lambda+\epsilon-\lambda\epsilon$$

According to the result provided in (15) and (16), it is known that $(M+N)=O(T^2)$, $2(M+N)=O(T^2)$.

II. When $\sigma(k)=0$

$$u_1(k)=-(GB)^{-1}[GB\widehat{f}_{\mathrm{m}}(k)+G\widehat{f}_{\mathrm{u}}(k)-Gx(k)] \tag{25}$$

According to (10)

$$\sigma(k)=Gx(k)-Gx(0)+h(k)=0 \tag{26}$$

in this case. So (25) can be written as

$$u_1(k)=-\widehat{f}_{\mathrm{m}}(k)-(GB)^{-1}(G\widehat{f}_{\mathrm{u}}(k)+h(k)-Gx(0)) \tag{27}$$

Substituting (27) into (14) gives

$$\sigma(k+1)=(GB)(f_{\mathrm{m}}(k)-\widehat{f}_{\mathrm{m}}(k))+G(f_{\mathrm{u}}(k)-\widehat{f}_{\mathrm{u}}(k)) \tag{28}$$

Considering (15) and (16), it can be concluded that

$$\sigma(k+1)=O(T^2) \tag{29}$$

The stability analysis of the closed loop behaviour is provided in the next section. □

Remark 3: In practical cases, it is possible that we have little knowledge about $x(0)$. The assumption that $x(0)=0$ is usually not problematic. If $x(0)$ in (10) can be ignored when (17) still holds, controller (20) promises the existence of reaching mode.

In the cases where the assumption about $x(0)$ is not accurate ($\widehat{x}(0) \neq x(0)$, with $\widehat{x}(0)$ representing the guess of $x(0)$), letting $k=0$ in (10)

$$\sigma(0)=Gx(0)-G\widehat{x}(0)+h(0) \neq 0$$

which means the sliding variable does not start from the sliding surface. However, this inaccuracy does not affect the form of (17) because the $Gx(0)$ entries in both (10) and (14) are replaced by $G\widehat{x}(0)$. As a result, the controller design method in Proposition 1 still applies. As proved above, this controller promises that the sliding variable moves towards the sliding surface no matter what the initial value of the sliding variable is. Therefore even though the sliding variable does not start from the sliding surface at $k=0$, a quasi-sliding mode could be reached afterwards (as proved above).

IET Control Theory Appl., 2010, Vol. 4, Iss. 10, pp. 2071–2081
doi: 10.1049/iet-cta.2009.0558

3.3 Closed loop behaviour on the sliding surface

In this section, we discuss the closed-loop performance of the system while travelling along the sliding surface.

Substituting (13) and (20) into (8), the closed-loop dynamic is derived as follows

$$\begin{aligned} x(k+1) &= Ax(k) + B(u_0(k) + u_1(k) + f_m(k)) + f_u(k) \\ x(k+1) &= Ax(k) + B(f_m(k) - \widehat{f_m}(k)) + Bu_0(k) + B(GB)^{-1} \\ &\quad \times Gx(0) + (f_u(k) - B(GB)^{-1}G\widehat{f_u}(k)) - B(GB)^{-1}h(k) \end{aligned} \tag{30}$$

From (10), we have

$$h(k) = \sigma(k) - Gx(k) + Gx(0) \tag{31}$$

So (30) can be written as (32) considering $u_0(k) = -Kx(k)$ and (31)

$$\begin{aligned} x(k+1) = (A - BK)x(k) &+ B(f_m(k) - \widehat{f_m}(k)) \\ &+ (f_u(k) - B(GB)^{-1}G\widehat{f_u}(k)) \\ &- B(GB)^{-1}(\sigma(k) - Gx(k)) \end{aligned} \tag{32}$$

Substituting (28) into the above gives

$$\begin{aligned} x(k+1) = (A + B(GB)^{-1}G - BK)x(k) &+ B[f_m(k) - 2\widehat{f_m}(k) \\ &+ \widehat{f_m}(k-1)] + [f_u(k) - 2B(GB)^{-1}G\widehat{f_u}(k) \\ &+ B(GB)^{-1}G\widehat{f_u}(k-1)] \end{aligned} \tag{33}$$

It can be seen in (33) that the uncertainties affect the closed loop system. To make sure that (33) is stable, the following conditions have to be considered. Taking (15) and (16) into account, (33) is written as (34)

$$\begin{aligned} x(k+1) = (A + B(GB)^{-1}G - BK)x(k) &+ B[f_m(k) \\ &- 2f_m(k-1) + f_m(k-2)] + [f_u(k) - 2B(GB)^{-1} \\ &\times Gf_u(k-1) + B(GB)^{-1}Gf_u(k-2)] \end{aligned} \tag{34}$$

Due to the assumption that both $f_m(k)$ and $f_u(k)$ are bounded, we can also assume that

$$\begin{aligned} -W \le B[f_m(k) - 2f_m(k-1) + f_m(k-2)] + [f_u(k) \\ -2B(GB)^{-1}Gf_u(k-1) + B(GB)^{-1}Gf_u(k-2)] = w(k) \le W \end{aligned} \tag{35}$$

with $0 < W < \infty$.

From (35), the closed loop dynamic can be represented by (36)

$$x(k+1) = (A + B(GB)^{-1}G - BK)x(k) + w(k) \tag{36}$$

K must be selected so that $\bar{\rho}_{max} \le 1$ with $\bar{\rho}_{max}$ standing for the spectral radius of $A + B(GB)^{-1}G - BK$.

Accordingly

$$\begin{aligned} x^T(k)[x(k+1) - x(k)] &= x^T(k)(A + B(GB)^{-1}G \\ &\quad - BK - I)x(k) + x^T(k)w(k) \\ &\le \rho_{max}x^T(k)x(k) + \|x^T(k)w(k)\| \\ &\le \rho_{max}\|x(k)\|^2 + \|x^T(k)W\| \end{aligned} \tag{37}$$

where ρ_{max} represents the spectral radius of the square matrix $A + B(GB)^{-1}G - BK - I$.

Remark 4: It can be seen that it is necessary to have $\rho_{max} \le 1$ to ensure the stability of the states.

Proposition 2: For system (8) for which the term containing uncertainties $W \neq 0$, with the sliding surface defined in (10) and (11) and controller proposed in Proposition 1, the final values of the system states stay within a band around the origin with the band width b where

$$b \le -\frac{W}{\rho_{max}} \tag{38}$$

Proof: As shown in (37), when $\|x(k)\| \ge -(W/\rho_{max}, \rho_{max}) < 0$, we have $x^T(k)[x(k+1) - x(k)] \le 0$. This means that as long as $x(k)$ travels beyond the band with an upper bound of the bandwidth $-(W/\rho_{max})$, it starts to move towards the origin until it enters the band mentioned above. Hence, it can be concluded that the the final states of the system are within this band. It should be noted that if the system is not affected by any uncertainty, which means W in (37) is zero, a negative ρ_{max} is sufficient to ensure the asymptotic stability of the closed-loop system. In the case where W is non-zero, the larger W is, the more negative ρ_{max} must be to guarantee stability. According to the definition of W in (35), the value of W is normally small if the sampling interval is well chosen as the uncertainties are assumed to be smooth functions. This leads to the conclusion that for a fixed W, the more negative ρ_{max} is, the narrower the band is. □

Remark 5: $\rho_{max} = \bar{\rho}_{max} - 1$. So, when $\bar{\rho}_{max}$ is designed to decide K, Remark 4 must be considered at the same time.

4 Example and simulation results

4.1 System description and modelling

The structure of an INTECO overhead crane (laboratory process) is shown in Fig. 1. The cart weighing 0.94 kg travels along a rail which adds 2.6 kg. The mass of the payload is 0.84 kg. The maximum of the length of the lift-rope is about 40 cm. There are three sensors and three encoders installed which sense and encode the position of the rail, position of the cart on the rail and the swing angle of the payload, respectively. The rail and the cart are driven by separate DC motors. The third DC motor takes charge of the length of the lift-rope. Fig. 2 is the schematic diagram of the crane.

The overhead crane is described by a discrete linear model in this paper although its physical model is non-linear [In cases where the available model is continuous, (1)–(7) may be used to derive a discrete model in the form of (8)]. This nominal linear model, which is not affected by uncertainties

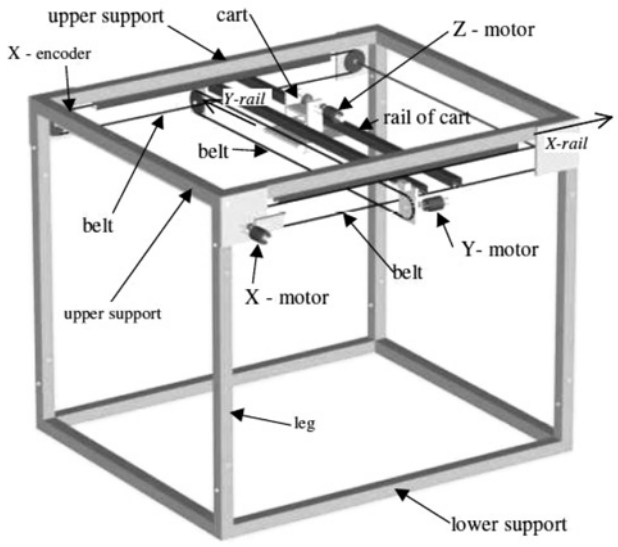

Figure 1 *INTECO overhead crane (courtesy: INTECO)*

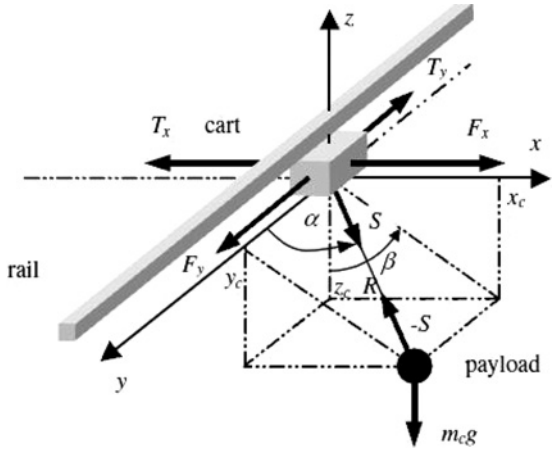

Figure 2 *Schematic structure of crane (courtesy: INTECO)*

is derived via multiple model least squares parameter estimation. Various sets of model structures (e.g. number of numerator/denominator coefficients) and parameters have been tested to guarantee that the selected model structure and parameters successfully reflect the system characteristics. First, models with different numbers of denominator and numerator coefficients are tried out. Then the model output was graphed against the experimental output to visually determine how well each model matched the experimental data. The numbers of denominator and numerator coefficients from the best fitting model was selected for the final model. Afterwards, denominator and numerator coefficients were estimated via least square method based on the structure of the model, which has been selected in the previous step [17]. The sampling frequency is chosen as 25 Hz. The identification is based on the data collected when the length of the rope is 50% of its maximum, whereas the variation of the length (if any) will be treated as an uncertainty in the controller design stage.

It is noticed that the motion of the crane actually contains two components, that is the horizontal motion (X direction) which is the motion of the cart on the rail and the motion of the rail in the vertical direction (Y direction). This means the system is multi-input and multi-output. It is noted that the cart and the rail are driven by separate motors so that the two motions can be separated in the identification process. The off-diagonal items in the multiple-input-multiple-output (MIMO) model, which represent the correlation between the two motions will be treated as an uncertain factor in the controller design process. The best structure of the system and the optimal set of parameters from the multiple model least squares parameter estimation are as follows

$$X \text{ direction: } \frac{y(k)}{u(k)} = \frac{0.381z^{-1} + 0.5435z^{-2} + 0.4484z^{-3} + 0.0064z^{-4}}{1 - 0.3823z^{-1} + 0.3706z^{-2} - 0.9777z^{-3}} \tag{39}$$

$$Y \text{ direction: } \frac{y(k)}{u(k)} = \frac{1}{1 + 0.3506z^{-1} + 0.1348z^{-2} - 0.6453z^{-3} - 0.6774z^{-4}} \tag{40}$$

with z representing the z-transform operator so that $y(k)z^{-q} = y(k-q)$ and setpoint filters for both directions are

$$\bar{s}_x(k) = 0.5s_x(k-1) + 0.5s_x(k-2) \tag{41}$$

$$\bar{s}_y(k) = 0.5s_y(k-1) + 0.5s_y(k-2) \tag{42}$$

with $s_{x/y}(k)$ representing the setpoints and $\bar{s}_{x/y}(k)$ the shaped setpoint [17]. Any cross-coupling between X and Y directions in the MIMO model simply adds to the uncertainties.

doi: 10.1049/iet-cta.2009.0558

Lemma 3: For $P \in R^{n\times m}$, (43) holds [12]

$$I_n = PP^{+} + P^{\perp}P^{\perp +} \tag{43}$$

with $P^{+} = (P^{\mathrm{T}}P)^{-1}P^{\mathrm{T}}$ and the columns of $P^{\perp} \in R^{n\times(n-m)}$ spanning the null space of P^{T}.

According to Lemma 1, f_x and f_y can be transformed as follows

$$f_x(k) = (B_x B_x^{+} + B_x^{\perp}B_x^{\perp +})f_x(k) = B_x f_{x\mathrm{m}}(k) + f_{x\mathrm{u}}(k) \tag{44}$$

$$f_y(k) = (B_y B_y^{+} + B_y^{\perp}B_y^{\perp +})f_y(k) = B_y f_{y\mathrm{m}}(k) + f_{y\mathrm{u}}(k) \tag{45}$$

with

$$f_{x\mathrm{m}}(k) = B_x^{+}f_x(k), f_{x\mathrm{u}}(k) = B_x^{\perp}B_x^{\perp +}f_x(k) \tag{46}$$

$$f_{y\mathrm{m}}(k) = B_y^{+}f_y(k), \quad f_{y\mathrm{u}}(k) = B_y^{\perp}B_y^{\perp +}f_y(k) \tag{47}$$

Consequently, the discrete state space descriptions of the system are

$$\begin{aligned} X \text{ direction: } x_x(k+1) &= A_x x_x(k) + B_x \Delta u_x(k-1) \\ &\quad + B_x f_{x\mathrm{m}}(k) + f_{x\mathrm{u}}(k) \end{aligned} \tag{48}$$

$$\begin{aligned} Y \text{direction: } x_y(k+1) &= A_y x_y(k) + B_y \Delta u_y(k-1) \\ &\quad + B_y f_{y\mathrm{m}}(k) + f_{y\mathrm{u}}(k) \end{aligned} \tag{49}$$

with

$$\begin{aligned} x_x(k) = \big[& e_x z^{-1} \quad e_x z^{-2} \quad e_x z^{-3} \quad e_x z^{-4} \quad \Delta u_x z^{-2} \\ & \Delta u_x z^{-3} \quad \Delta u_x z^{-4} \quad \Delta s_x z^{-1} \quad \Delta s_x z^{-2} \quad \Delta s_x z^{-3} \\ & \Delta s_x z^{-4} \quad \Delta s_x z^{-5} \big] \end{aligned}$$

$$\begin{aligned} x_y(k) = \big[& e_y z^{-1} \quad e_y z^{-2} \quad e_y z^{-3} \quad e_y z^{-4} \quad e_y z^{-5} \quad \Delta u_y z^{-2} \\ & \Delta u_y z^{-3} \quad \Delta u_y z^{-4} \quad \Delta u_y z^{-5} \quad \Delta u_y z^{-6} \quad \Delta s_y z^{-1} \\ & \Delta s_y z^{-2} \quad \Delta s_y z^{-3} \quad \Delta s_y z^{-4} \quad \Delta s_y z^{-5} \quad \Delta s_y z^{-6} \big] \end{aligned}$$

$A_x \in R^{12\times 12}$, $B_x \in R^{12\times 1}$, $f_{x\mathrm{m}} \in R$, $f_{x\mathrm{u}} \in R^{12\times 1}$, $A_y \in R^{16\times 16}$, $B_y \in R^{16\times 1}$, $f_{y\mathrm{m}} \in R$, $f_{y\mathrm{u}} \in R^{16\times 1}$ and Δ represents the difference operator, that is $\Delta a(k) = a(k+1) - a(k)$. $e_{x/y}(k) = y_{x/y}(k) - \bar{s}_{x/y}(k)$. The setpoints are filtered to shape the trajectory of the X and Y motions and the control object is to reduce to 0 the error between the respective filtered values and the relevant positions. Furthermore, let f_x and f_y denote the total uncertainties (which include ones incurred by the friction and swing of the payload, etc.) in the X and Y directions, respectively. It is not inappropriate to judge that the uncertainties are all smooth and bounded as required in Section 2. The present values of these uncertainties are unknown but their past values may be sensed or derived from the physical model. The sequences of error signals $e_{x/y}$ are contained in the state vectors so that the position of the cart or rail will be forced to follow their setpoints as the control actions drive the state vectors to the vicinity of the origin.

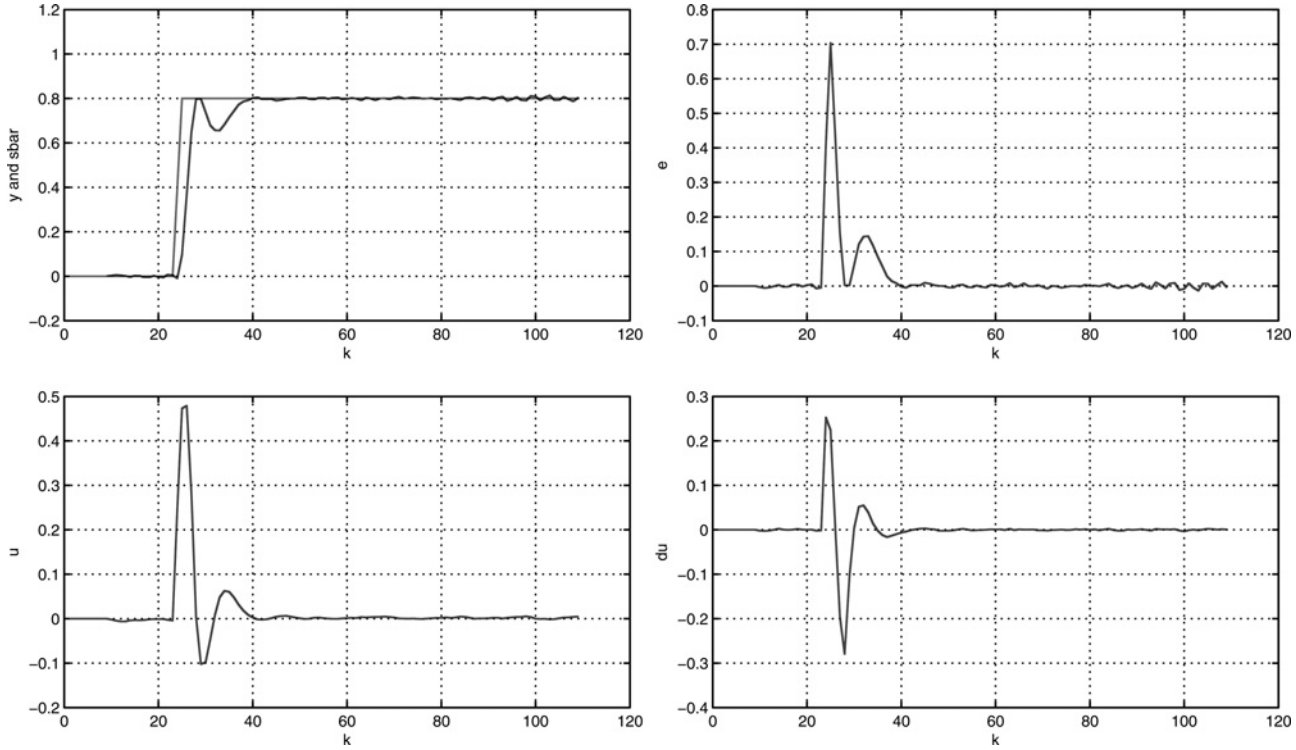

Figure 3 *Simulation: cart position*

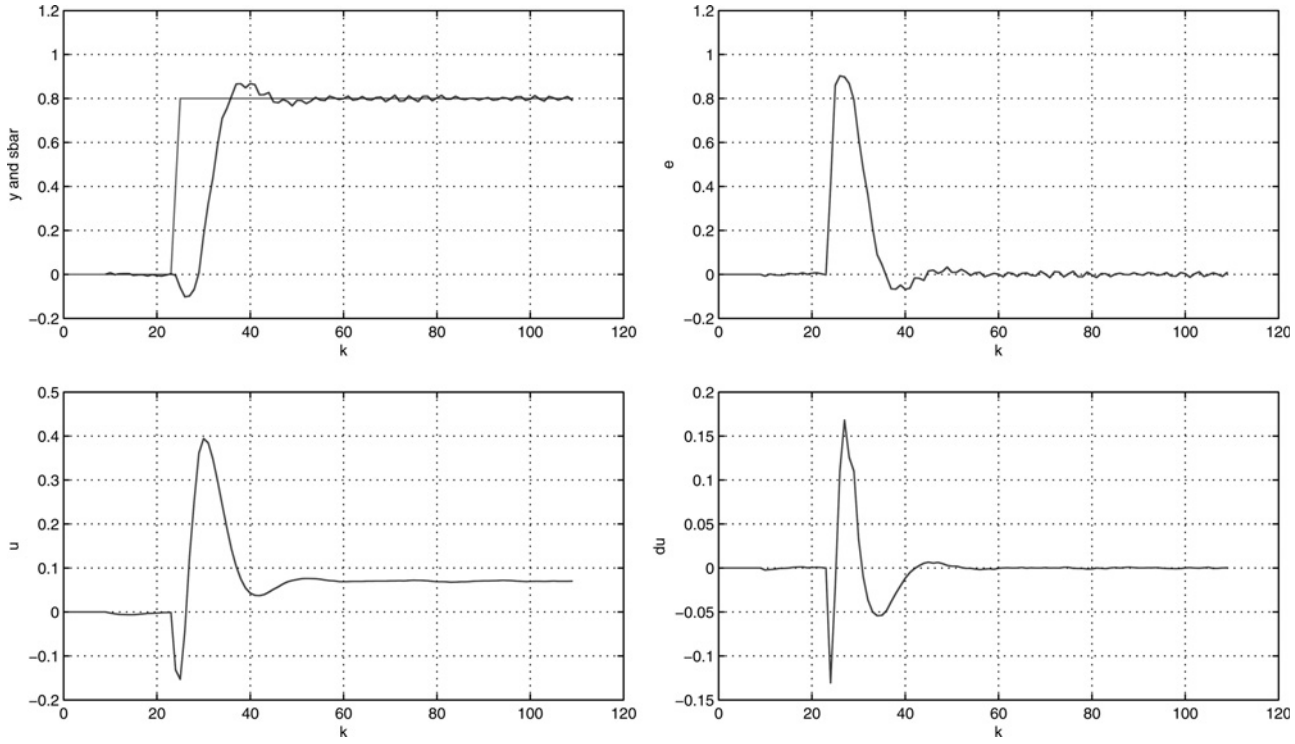

Figure 4 *Simulation: rail position*

4.2 Simulation and experimental results

4.2.1 Simulation results: Based on the model derived above, the ISMC controller is designed according to Section 3. K could be designed via any traditional method as long as the statement in Remark 4 is satisfied. Here, a discrete linear quadratic regulator is adopted. $u_1(k)$ is designed following Proposition 1. ϵ is chosen as 0.5 and λ is chosen as 0.7 according to Proposition 1. The simulation is run with a sampling interval 0.04 s, which is consistent with the identification process.

Fig. 3 shows the trajectories of the position of the cart on the rail (X direction) and its setpoint, the error signal and also the control signal.

Fig. 4 shows the trajectories of the position of the rail (Y direction) and its setpoint, the error signal as well as the control signal.

It can be seen that there are oscillations in both the figures due to the finite step size and the existence of unmatched uncertainties. But the cart and rail positions are forced to follow their shaped setpoint by the control action. In this simulation process, the uncertainties f_x and f_y are formulated as sums of sine and cosine functions with different frequencies. Their past values are used as the estimation of their current values. It is shown that the effects of the uncertainties are suppressed by the integral sliding mode controller proposed.

4.2.2 Experimental results: This experiment is performed using a Linux operating system with real time extensions (RTAI). The position of the cart and the rail are both scaled to $[-1, 1]$ in the driver program. Figures below are plotted based on encoded and scaled real process data.

Figs. 5 and 6 show the motion of the cart and rail, respectively, when the length of the rope is set to the same as the value used in the identification process. The controller applied to the hardware is the same one as used in the simulation process. However, as the values of all the

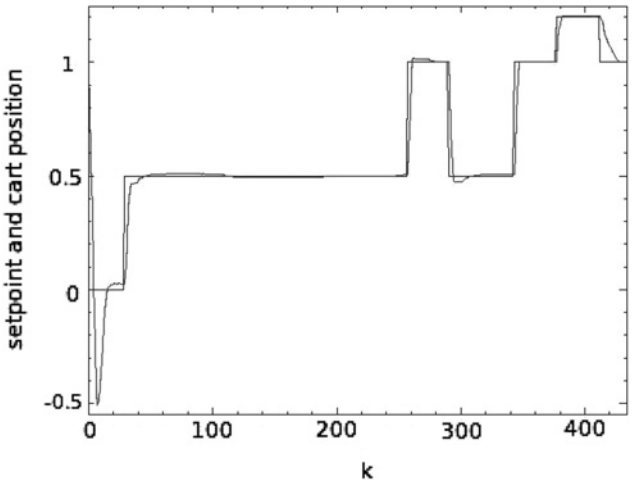

Figure 5 *Position of the cart and its setpoint*

doi: 10.1049/iet-cta.2009.0558

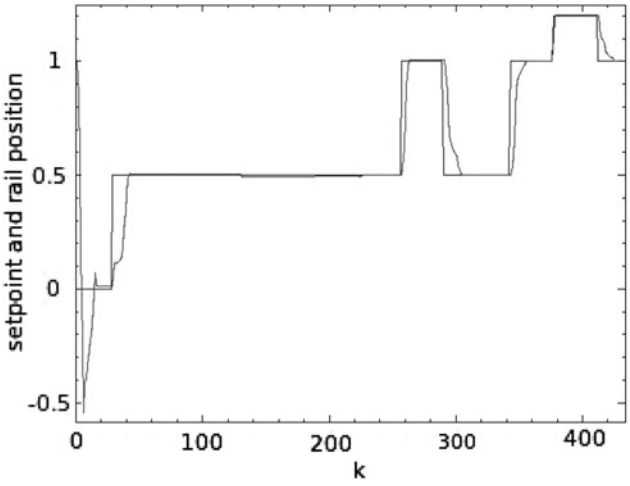

Figure 6 *Position of the rail and its setpoint*

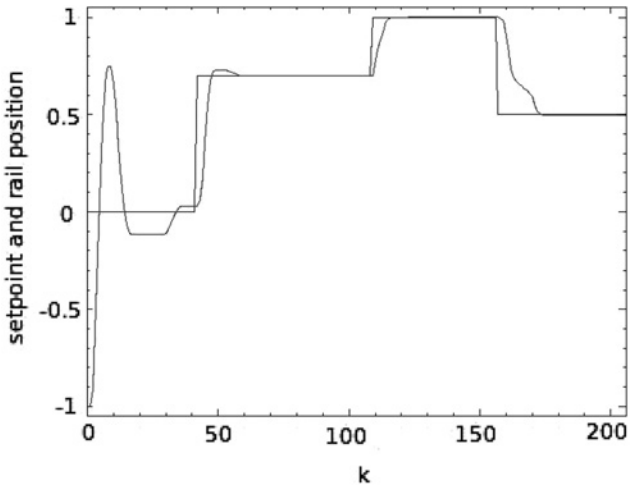

Figure 8 *Position of the rail and its setpoint, length of rope equals 1.2 times the nominal value*

variables returned by the sensors are properly scaled for simplicity and unity purpose, the control input is also scaled before being applied to the crane hardware. It is shown that the trajectories stay within a band around their setpoints which is consistent with the closed-loop behaviour analysis in Section 3. It should be noticed that the state vector mentioned in Section 3 refers to the one containing the error signal sequence in the experimental stage. Therefore the fact that the motion trajectories stay within a band around their setpoints is equivalent to the requirement that the state variables stay within a band around the origin.

Figs. 7–10 show the motion of the cart and rail, respectively, when the length of the rope is adjusted manually to values, which differ from the one used in the identification process, that is an unmodelled uncertainty is added. In Figs. 7 and 8, the real value of the length of the lift-rope is 120% of the nominal value and in Figs. 9 and 10, the real value is 87% of the nominal value. As happens often in real industrial processes, the overhead crane lifts the payload up from the origin and moves it to the destination where it puts it down. The 'up and down' actions are realised by changing the length of the lift rope. It is required that the control action is able to cope with such situations. It is seen from Figs. 7 to 10 that the system performance is roughly the same as the cases in Figs. 5 and 6. Superior robustness of the controller is shown in this trial. Fig. 11 shows the system response (position of the rail) while linear quadratic (LQ) controller is applied to the crane process with the length of the rope equal to its nominal value. It is seen that the response is roughly the same as that in Fig. 6. Although the length of rope is changed to 87% of the nominal value, the system under LQ controller is shown in Fig. 12 (position of the rail). It is obvious that LQ controller is not achieving a

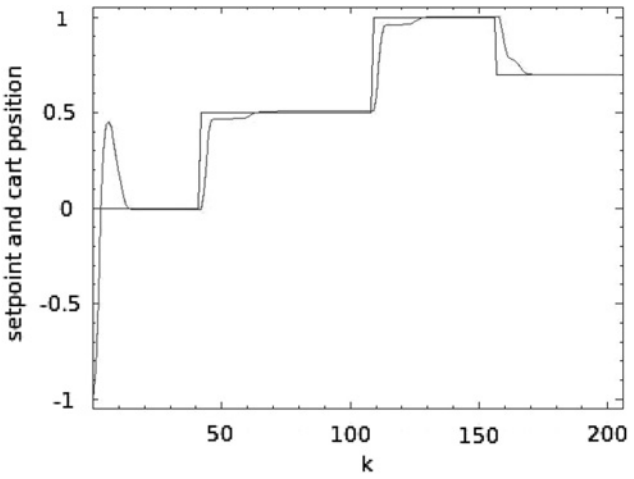

Figure 7 *Position of the cart and its setpoint, length of rope equals 1.2 times the nominal value*

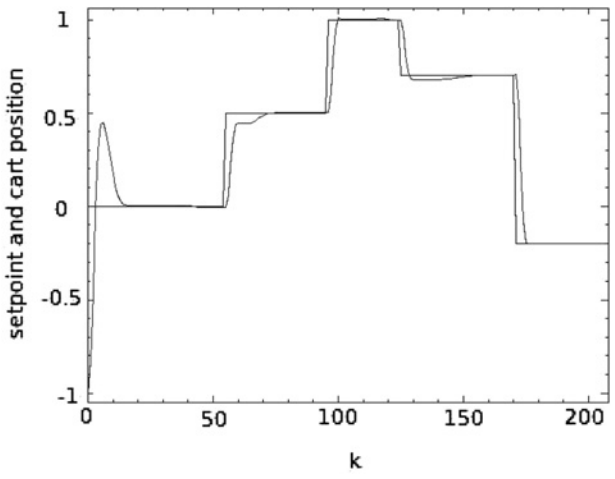

Figure 9 *Position of the cart and its setpoint, length of rope equals 0.87 times the nominal value*

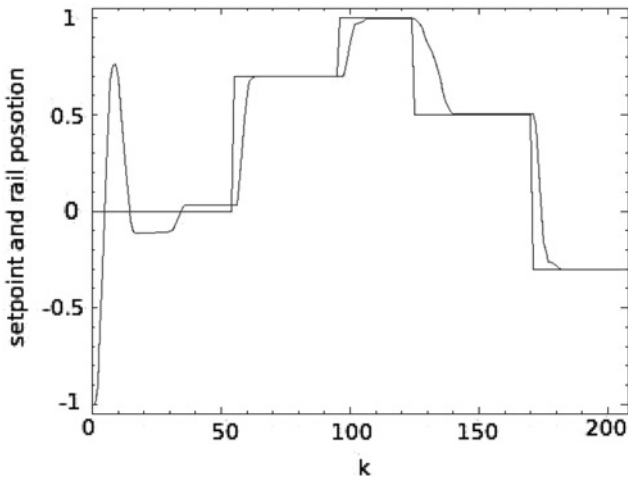

Figure 10 *Position of the rail and its setpoint, length of rope equals 0.87 times the nominal value*

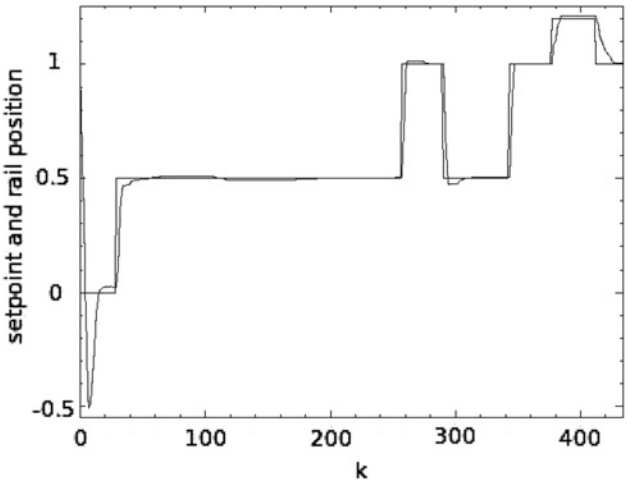

Figure 11 *Position of the rail and its setpoint when LQ controller is applied, length of rope equals its nominal value*

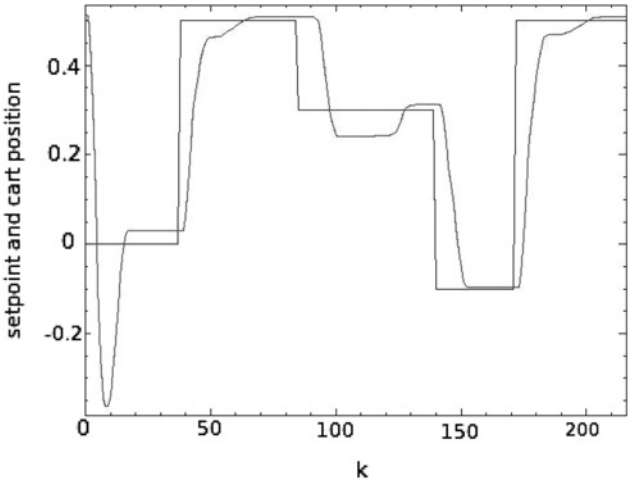

Figure 12 *Position of the rail and its setpoint when LQ controller is applied, length of rope equals 0.87 times the nominal value*

performance as good as integral sliding mode controller in case of large uncertainty.

5 Conclusion

In this paper, integral sliding mode control for overhead crane system is considered. In the controller design theory sections, matched and unmatched uncertainties in the continuous time counterpart of the system model are treated. The integral sliding mode controller is designed based on both the existent conditions of sliding mode and the stability conditions of the closed-loop behaviour during sliding. It is shown that the influence of the matched uncertainty is suppressed by the integral sliding mode controller. The system states stay within a band, the width of which depends on the size of the uncertainty and design parameters. The illustrative example provided in Section 4 validates the reported methods. Results from both simulation and on-line experiments are provided. It is shown that the overhead crane system is successfully controlled despite the existence of matched and unmatched uncertainties. The system trajectory stays within a band around the origin as proved in Section 3. Even in the presence of an unmodelled uncertainty (length of lift-rope changed), a satisfying performance is still achieved.

6 References

[1] MARTINDALE S.C., DAWSON D.WI., ZHU J., RAHN C.D.: 'Approximate nonlinear control for a two degree of freedom overhead crane: theory and experimentation'. Proc. American Control Conf., Seattle, Washington, June 1996, pp. 301–305

[2] SAKAWA Y., SANO H.: 'Nonlinear model and linear robust control of overhead travelling cranes'. Proc. Second World Congress of Nonlinear Analysts, 1997, pp. 2197–2207

[3] PIAZZI A., VISI A.: 'Optimal dynamic-inversion-based control of an overhead crane', *IEE Proc. Control Theory Appl.*, 2002, **149**, (5), pp. 405–412

[4] CHANG C.Y.: 'Adaptive fuzzy controller of the overhead cranes with nonlinear disturbance', *IEEE Trans. Ind. Inf.*, 2007, **3**, (2), pp. 164–172

[5] UTKIN V.I.: 'Variable structure systems with sliding modes', *IEEE Trans. Autom. Control*, 1977, **AC-22**, (2), pp. 212–222

[6] EDWARDS C., SPURGEON S.K.: 'Sliding mode control, theory and applications' (CRC Press, Taylor & Francis Group, 1998)

[7] DECARLO R.A., ZAK S.H., MATTHEWS G.P.: 'Variable structure control of nonlinear multivariable systems: a tutorial', *Proc. IEEE*, 1988, **76**, (3), pp. 212–232

doi: 10.1049/iet-cta.2009.0558

[8] GAO W., WANG Y., HOMAIFA A.: 'Discrete-time variable structure control systems', *IEEE Trans. Ind. Electron.*, 1995, **42**, (2), pp. 117–122

[9] UTKIN V.I., SHI J.: 'Integral sliding mode in systems operating under uncertainty conditions'. Proc. 35th Conf. on Decision and Control, Kobe, Japan, December 1996, pp. 4591–4956

[10] WANG J.D., LEE T.L., JUANG Y.T.: 'New methods to design an integral variable structure controller', *IEEE Trans. Autom. Control*, 1996, **41**, (1), pp. 140–143

[11] ACKERMANN J., UTKIN V.I.: 'Sliding mode control design based on ackermann's formula', *IEEE Trans. Autom. Control*, 1998, **43**, (2), pp. 234–237

[12] CASTANOS F., FRIDMAN L.: 'Analysis and design of integral sliding manifolds for systems with unmatched perturbations', *IEEE Trans. Autom. Control*, 2006, **51**, (5), pp. 853–858

[13] CAO W.J., XU J.X.: 'Nonlinear integral-type sliding surface for both matched and unmatched uncertain systems', *IEEE Trans. Autom. Control*, 2004, **49**, (8), pp. 1355–1360

[14] WANG B., YU X., CHEN G.: 'ZOH discretization effect on single-input sliding mode control systems with matched uncertainties', *Automatica*, 2009, **45**, pp. 119–125

[15] ABIDI K., XU J.X., YU X.: 'On the discrete-time integral sliding-mode control', *IEEE Trans. Autom. Control*, 2007, **52**, (4), pp. 709–715

[16] SU W.C., DRAKUNOV S.V., OZGUNER U.: 'An $O(T^2)$ boundary layer in sliding mode for sampled-data systems', *IEEE Trans. Autom. Control*, 2000, **45**, (3), pp. 482–485

[17] WEI B.N.: 'An innovative approach to overhead crane control'. Bachelor's Degree thesis, University of New South Wales, 2008